

Supporting Information for

Impact of seawater inorganic carbon chemistry on element incorporation in foraminiferal shell carbonate

S. Karancz¹; L. J. de Nooijer¹; G. J. A. Brummer¹; J. Lattaud²; N. Haghipour^{2,3}; Y. Rosenthal⁴; G. J.

Reichert^{1,5}

¹NIOZ-Royal Netherlands Institute for Sea Research, Texel, Netherlands

²Department of Earth Sciences, Biogeoscience Group, ETH Zürich, Zürich, Switzerland

³Laboratory of Ion Beam Physics, ETH Zürich, Zürich, Switzerland

⁴Department of Marine and Coastal Sciences, Rutgers University, State University of New Jersey, New Brunswick, NJ, USA

⁵Department of Earth Sciences, Utrecht University, Utrecht, Netherlands

Introduction

This supplementary information file contains the following texts and figures:

Text S1: Radiocarbon Determinations

Text S2: Elevated foraminiferal Mg/Ca values in the Mediterranean Sea

Figure S1: Calibration of radiocarbon ages

Figure S2: Pyrite precipitation inside the foraminifera's shell

Figure S3: Cross section image of *T. sacculifer* overlaid by the Mg/Ca profile

Figure S4: Residuals of Mg/Ca

Figure S5: Foraminiferal Mg/Ca vs. temperature

Figure S6: Temperature and salinity corrected residual Mg/Ca

Figure S7: B/Ca of *G. bulloides*, *T. sacculifer*, *G. ruber albus*, and *N. incompta* vs. $[\text{CO}_3^{2-}]$

Figure S8: Residual S/Ca vs. $[\text{CO}_3^{2-}]$

Figure S9: Foraminiferal S/Ca vs. Mg/Ca

Figure S10: Foraminiferal S/Ca vs. Sr/Ca

Text S1: Radiocarbon Determinations

80–100 well preserved shells of *G. bulloides* were used for each sample. Radiocarbon determinations ($^{14}\text{C}/^{12}\text{C}$) were performed with a gas ion source in a Mini Carbon Dating System at the Laboratory of Ion Beam Physics, ETH Zürich, with an automated method for acid digestion of carbonates (Wacker et al., 2013). Briefly, vials (septa sealed 4.5 ml exetainers vials from Labco Limited, UK) containing the samples were purged for 10 min with a flow of 60 mL min^{-1} of helium to remove atmospheric CO_2 . Following that step, samples were briefly leached by adding $100\text{ }\mu\text{L}$ of ultrapure HCl (0.02 M) with an automated syringe to remove possible surface contaminants. The CO_2 released from the sample, referred to as leachate was transported by helium to a zeolite trap and automatically injected into the ion source to be measured for radiocarbon. The remaining sample, containing $> 10\text{ }\mu\text{g C}$ and referred to as leached sample, was subsequently acidified by adding $100\text{ }\mu\text{L}$ of ultrapure H_3PO_4 (85%) that was heated to $60\text{ }^\circ\text{C}$ for at least 1 hr. The released CO_2 was loaded in a second trap and injected into the ion source to be analyzed (Wacker et al., 2014). Difference between the leached and leachate values were $< 5\%$ which is an indication of near complete removal of surface contaminants. Radiocarbon determinations were corrected for isotopic fractionation via $^{13}\text{C}/^{12}\text{C}$ isotopic ratios and are given in conventional radiocarbon ages.

Text S2: Elevated foraminiferal Mg/Ca values in the Mediterranean Sea

Foraminiferal Mg/Ca values show progressive increase in the Mediterranean Sea from the West to the East, that may (at least partly) be associated with a post depositional diagenetic overprint, (Hover et al., 2001; Kozdon et al., 2013; Ni et al., 2020; Panieri et al., 2017; Sexton et al., 2006; Stainbank et al., 2020), possibly from the high saturation state of pore fluids. Deposition of a diagenetic secondary inorganic calcite layer may result in elevated Mg concentrations, increasing overall shell values to values as high as 30 mmol mol^{-1} (Boussetta et al., 2011; Regenberg et al., 2007). Although extensive cleaning procedures involving partial calcite dissolution can be applied, this may only partially remove these contaminant, high-Mg phases (Barker et al., 2003). Compared to expected Mg/Ca values calculated using local sea surface temperatures and calibrations from Anand et al. (2003), Dekens et al. (2002), Mashiotta et al. (1999), and Nürnberg et al. (1996), we observe Mg/Ca values in the Eastern Mediterranean that are 5-6 times higher. Although this offset is somewhat reduced when Mg/Ca values are corrected for the effect of pH, and salinity (Gray & Evans, 2019), Mg/Ca (or corresponding temperatures) remain too high, hinting at additional factors affecting Mg uptake and/or contamination (Supporting Figure S3).

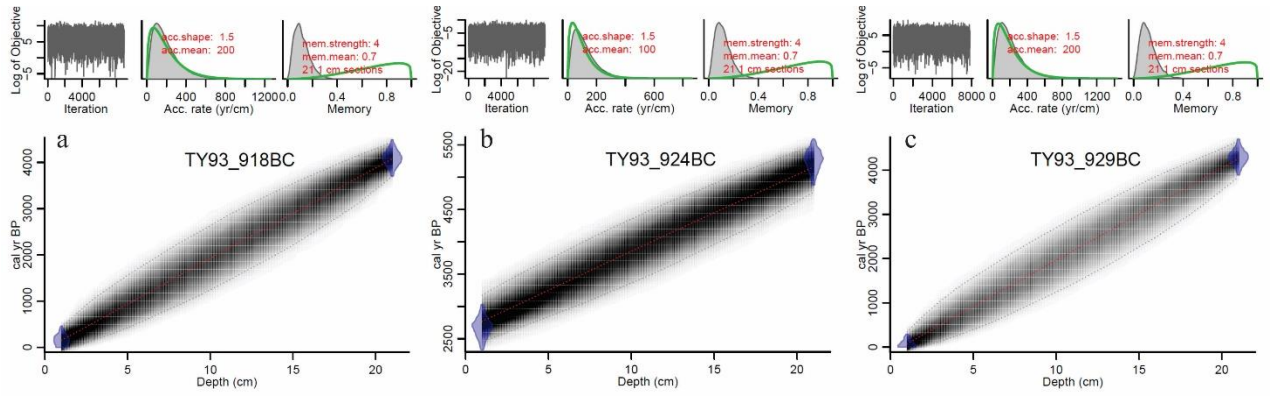


Figure S1. Calibrated radiocarbon ages of the sediment cores a) TY93-918, b) TY93-924, and c) TY93-929 versus core depth show the Holocene age of the core tops. The age-depth model was computed using Bayesian age-depth modelling in the Bacon v2.3 package for the R statistical programming software (Blaauw & Christen, 2011).

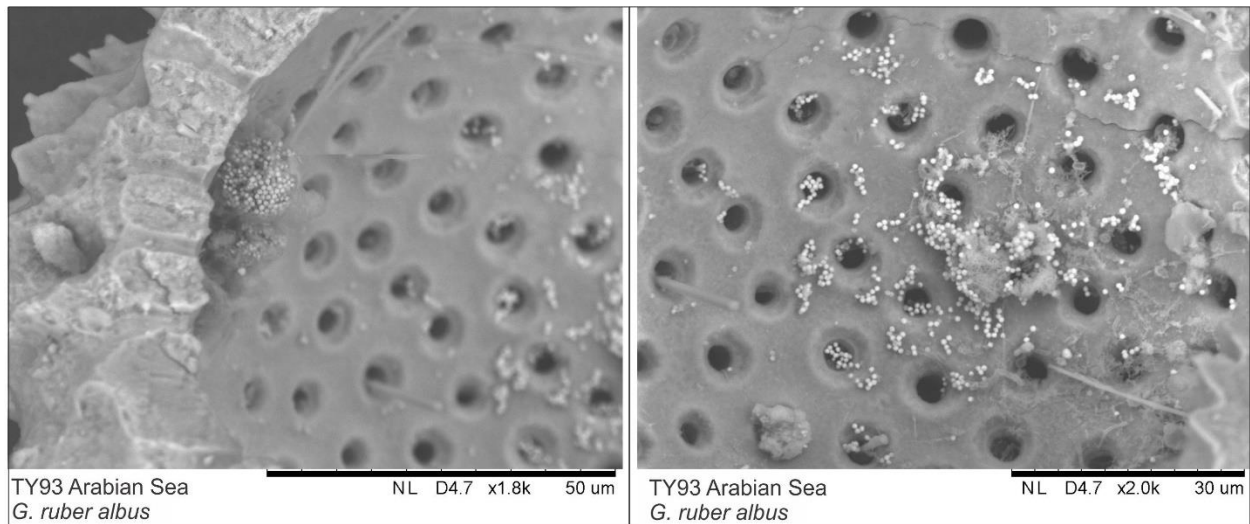


Figure S2. Scanning Electron Microscope images are shown as examples of pyrite precipitation inside the foraminifera's shell from the Arabian Sea. Samples with pyrite inside or outside of the shells were excluded from the dataset.

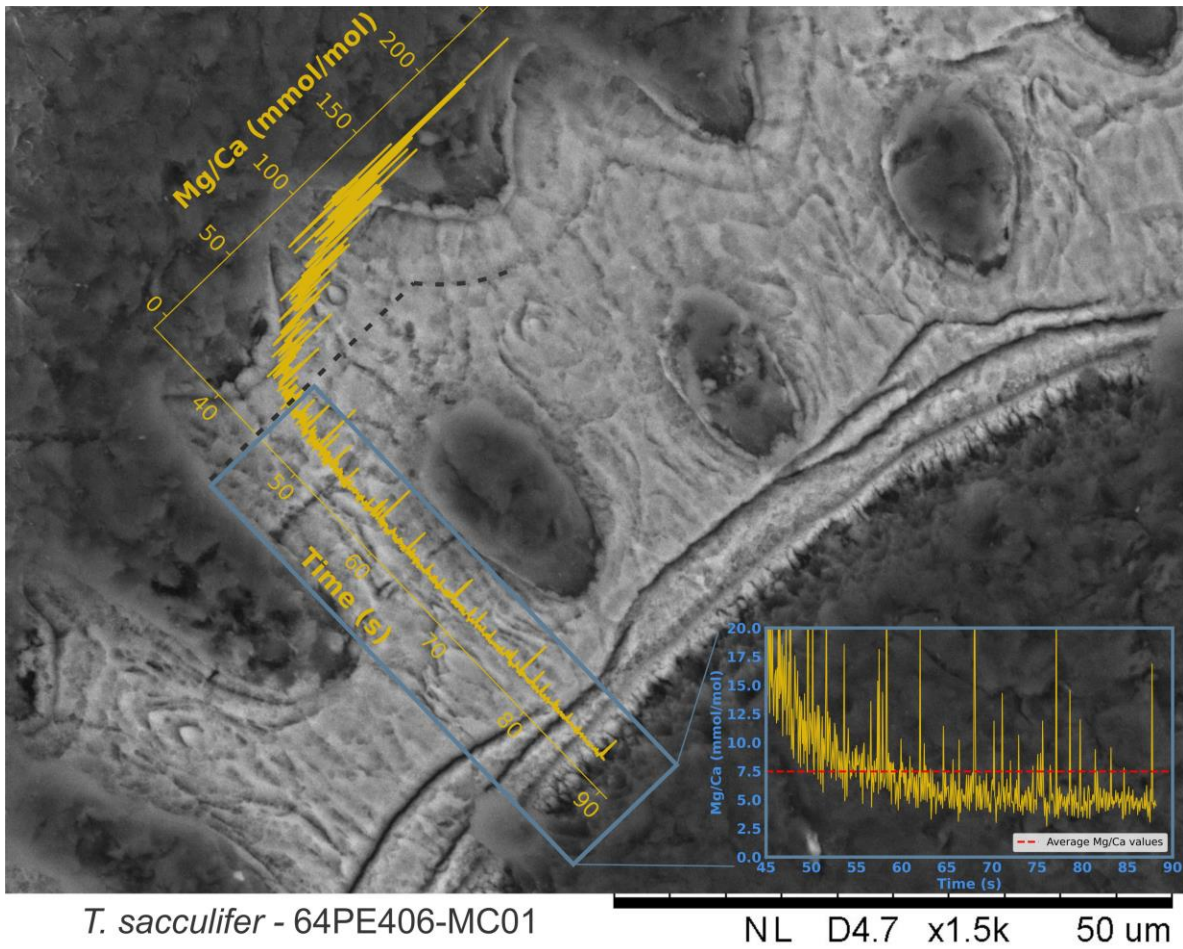


Figure S3. Scanning electron microscope (SEM) image of the final chamber of an embedded, polished and etched specimen of *T. sacculifer* from the Eastern Mediterranean (64PE406-MC01). The cross section image is overlaid by the Mg/Ca profile of the same chamber measured by LA-ICP-MS. The black dashed line indicates the likely transition of inorganic and biogenic carbonates.

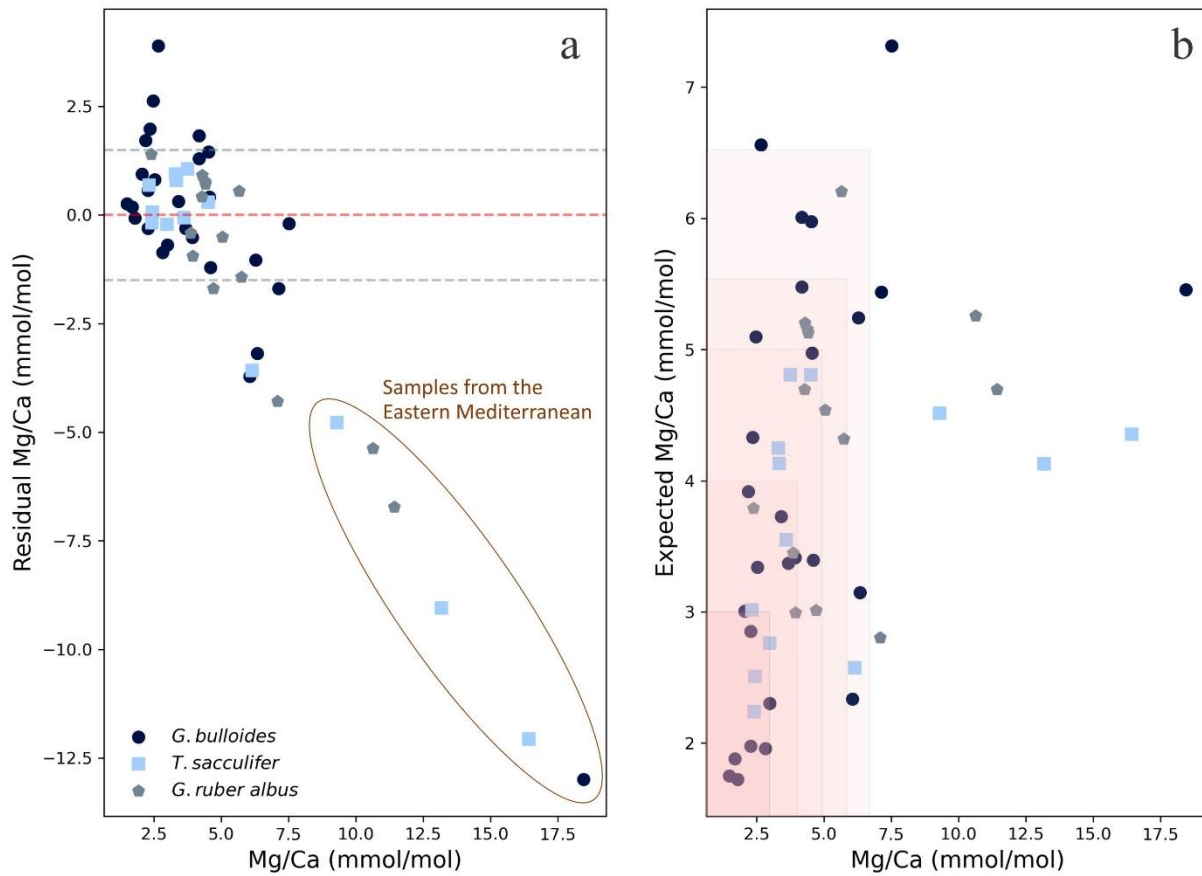


Figure S4. Mg/Ca residuals (a) and expected Mg/Ca values (b) calculated using the calibrations of Gray and Evans (2019) plotted against measured Mg/Ca ratios of *G. bulloides*, *T. sacculifer*, and *G. ruber albus*. Residual Mg/Ca values express the offset between the expected Mg/Ca values based on temperature, salinity and pH of the corresponding site. Samples showing an offset larger than 4.5 mmol/mol compared to the expected Mg/Ca values are here considered to be affected by diagenesis and therefore excluded from further analysis in this study .

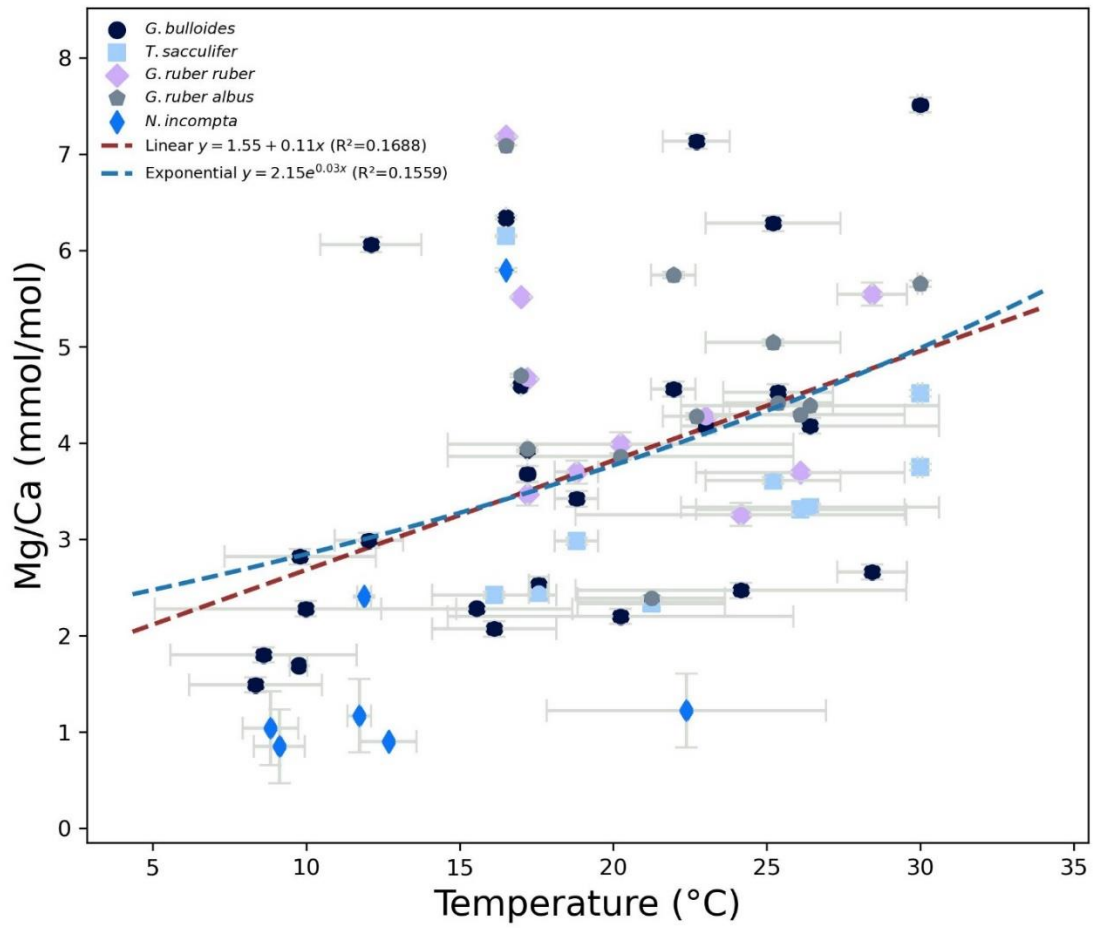


Figure S5. Mg/Ca values plotted against temperature fitted with linear (red dashed line, $p < 0.001$) and exponential curve (blue dashed line, $p < 0.001$, where p -value was calculated after log transformation) .

Temperature and salinity corrected

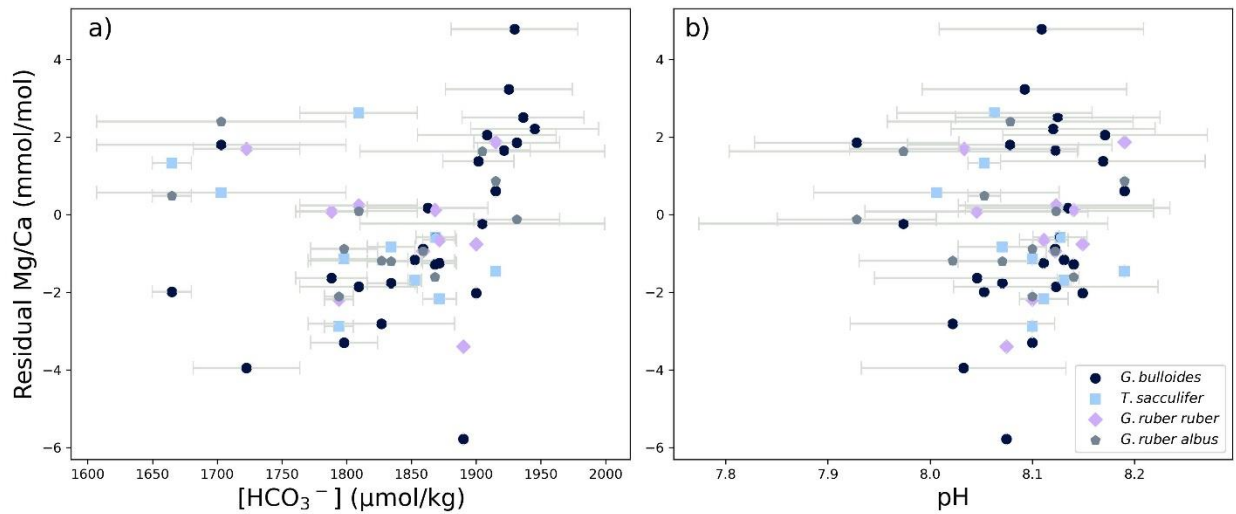


Figure S6. Residuals of Mg/Ca calculated from the temperature and salinity dependencies plotted against seawater a) $[\text{HCO}_3^-]$ and b) pH.

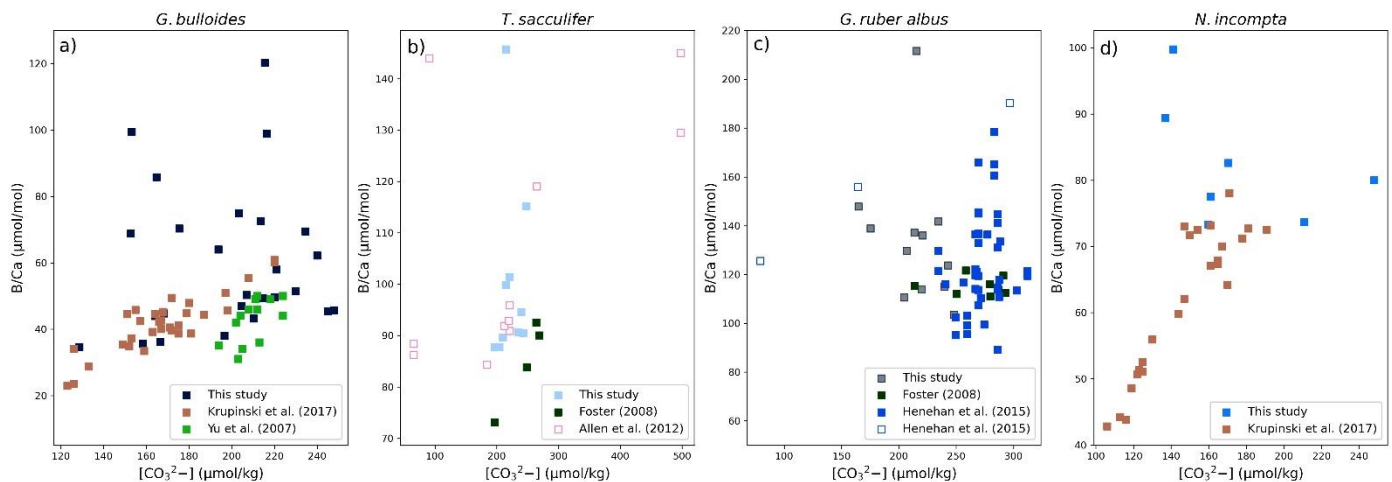


Figure S7. B/Ca of a) *G. bulloides*, b) *T. sacculifer*, c) *G. ruber albus*, and d) *N. incompta* plotted against seawater $[\text{CO}_3^{2-}]$ in comparison with the data from Allen et al. (2012), Foster (2008), Henehan et al. (2015), Krupinski et al. (2017), Yu et al. (2007). Empty squares mark results from culture experiments (Allen et al., 2012; Henehan et al., 2015).

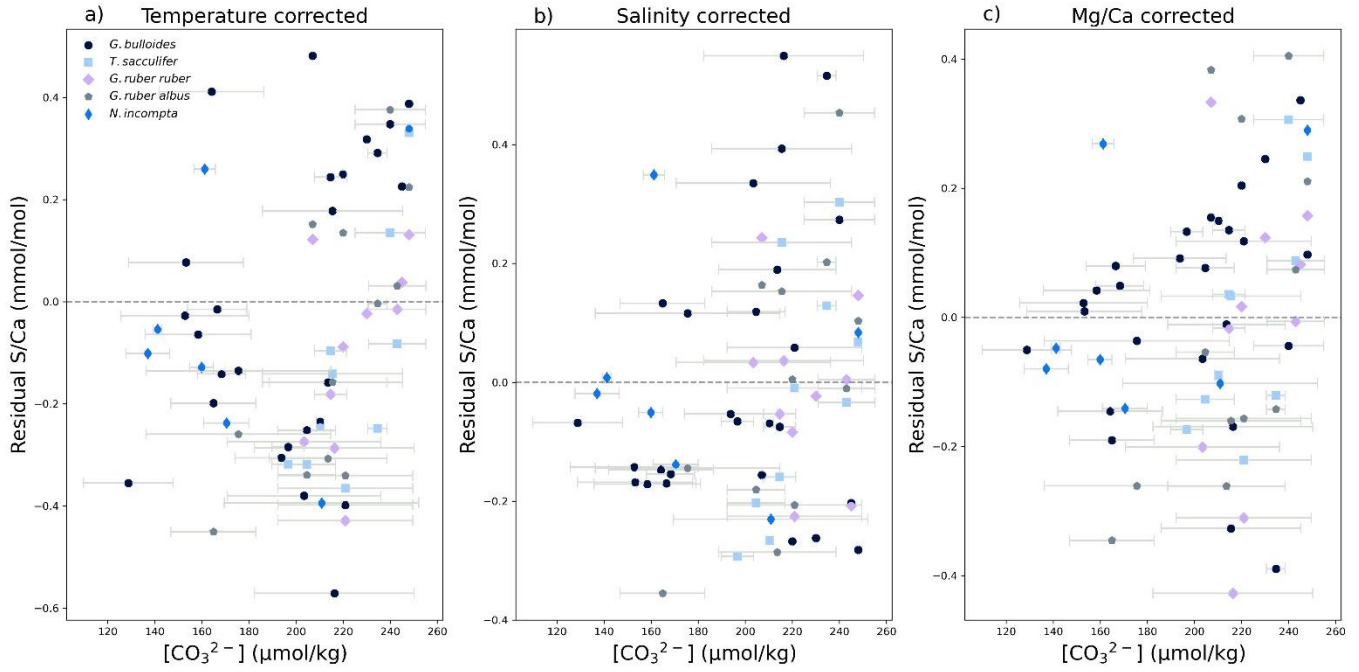


Figure S8. Residuals of S/Ca calculated from a linear regression with a) temperature, b) salinity and c) Mg/Ca and plotted against $[CO_3^{2-}]$.

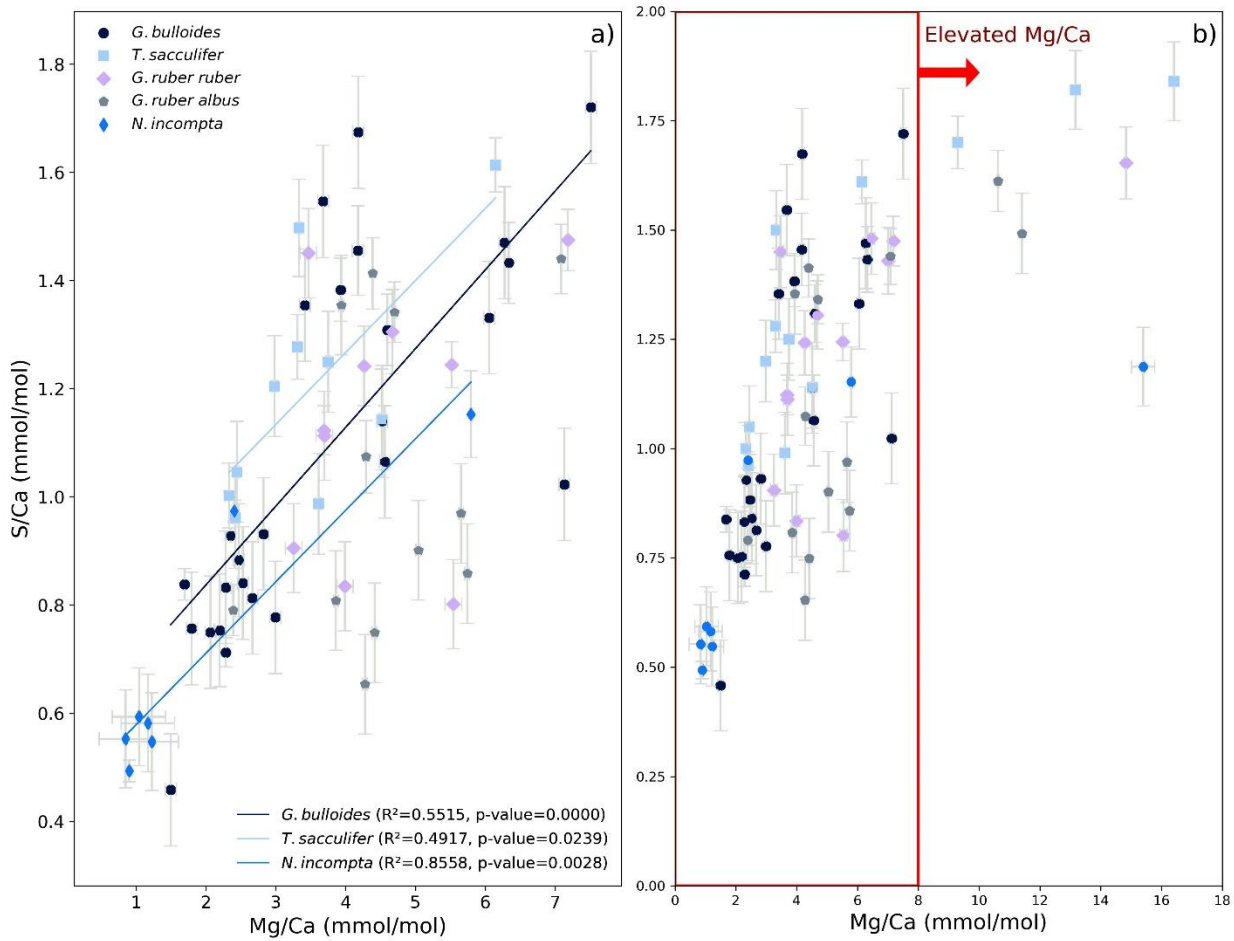


Figure S9. Foraminiferal S/Ca values plotted against Mg/Ca values a) excluding samples from the Eastern Mediterranean and fitted with linear regression lines when $p\text{-value} < 0.05$ b) including samples with elevated Mg/Ca values from the Easter Mediterranean. Error bars indicate $\pm 1\sigma$ uncertainties derived from duplicate analysis of the samples.

